1 # Occurrence and source apportionment of perfluoroalkyl acids
2 # (PFAAs) in the atmosphere in China

3 Deming Han[1], Yingge Ma[2], Cheng Huang[2], Xufeng Zhang[1], Hao Xu[1], Yong Zhou[1], Shan Liang[1],
4 Xiaojia Chen[1], Xiqian Huang[1], Haoxiang Liao[1], Shuang Fu[1], Xue Hu[1], Jinping Cheng[1]

5 [1] School of Environmental Science and Engineering, Shanghai Jiao Tong University, Shanghai 200240, China
6 [2] State Environmental Protection Key Laboratory of the Formation and Prevention of Urban Air Pollution Complex,
7 Shanghai Academy of Environmental Sciences, Shanghai 200233, China

8 *Correspondence to*: Jinping Cheng (jpcheng@sjtu.edu.cn)

9 **Abstract:**

10 Perfluoroalkyl acids (PFAAs) are a form of toxic pollutant that can be transported across the globe and accumulated in
11 the bodies of wildlife and humans. A nationwide geographical investigation considering atmospheric PFAAs was
12 conducted in China, which provides an excellent chance to investigate their occurences, spatial trends, and potential
13 sources. The total concentrations of thirteen PFAAs were 6.19–292.6 pg/m^3, with an average value of 39.8±28.1 pg/m^3,
14 which were higher than other urban levels but lower than point source measurements. Perfluorooctanoic acid (PFOA)
15 was the dominant PFAAs (20.6%), followed by perfluoro–hexanoic acid (PFHxA), perfluorooctane sulfonate (PFOS),
16 and perfluoro–heptanoic acid (PFPeA). An increasing seasonal trend of PFAAs concentrations was shown as summer <
17 autumn < spring < winter, which may be initiated by stagnant meteorological conditions. Spatially, the content of PFAAs
18 displayed a declining gradient trend of central areas > eastern areas > western areas, and Henan contributed as the largest
19 proportion of PFAAs. Four sources of PFAAs were identified using a positive matrix factorization (PMF) model,
20 including PFOS–based products (26.1%), PFOA–based, and PFNA–based products (36.6%), degradation products of
21 fluoro–telomere–based products (15.5%), and an unknown source (21.8%).

22

23 ## 1.Introduction

24 Perfluoroalkyl acids (PFAAs) are a class of ionic polyfluoroalkyl substances (PFASs), which have excellent
25 characteristics in terms of chemical and thermal stability, high surface activity, and water and oil repulsion (Lindstrom et
26 al., 2011;Wang et al., 2014). They are applied to a wide variety of domestic and industrial products such as textiles, oil
27 and liquid repellents, firefighting foam, pesticides, and food packaging materials (Xie et al., 2013;Wang et al., 2014).
28 PFAAs can be released to the surrounding environment during manufacturing and use of PFAAs containing products,

29   which are ubiquitous in the environment (e.g., in the atmosphere, water, or snow), in wildlife, and even in the human

30   body (Dreyer et al., 2009;Wang et al., 2017;Hu et al., 2016). PFAAs can change adult thyroid hormone levels, reduce

31   newborn birth weight, and biomagnify in the food chain, which can be extremely toxic to animals and humans (Hu et al.,

32   2016;Jian et al., 2017;Baard Ingegerdsson et al., 2010). Of the PFAAs, the long–chain (C ≥7) perfluoroalkyl carboxylic

33   acids (PFCAs) and (C ≥6) perfluoroalkyl sulfonic acids (PFSAs) are more toxic and bio–accumulative than their

34   short–chain analogues (Konstantinos et al., 2010). This especially applies to perfluorooctanoic acid (PFOA) and

35   perfluorohexane sulfonate (PFHxS) for which have been regulated in numerous countries, while perfluorooctane

36   sulfonate (PFOS) have been added to Annex B of the Stockholm Convention in 2009 (Johansson et al., 2008).

37   PFAAs can originate from direct sources of products' emissions as well as indirect sources of incomplete degradation of

38   their precursors. It is estimated that the global historical emission quantities of C4–C14 PFCAs were 2610–21400 t in the

39   period of 1951–2015, of which PFOA–based and perfluorononanoic–acid (PFNA)–based products contributed the most

40   (Wang et al., 2014). A trend of geographical distribution of major fluorochemical manufacturing sites has shifted from

41   Western Europe, US, and Japan to the emerging economies in the Asia Pacific area over the past decades. This is

42   especially true for China, which was the world's largest industrial contributor of PFOAs (50–80 t) and PFOS–related

43   compounds (~1800 t) in 2009 (Xie et al., 2013). PFOA– and PFOS– based products were added to the Catalogue for the

44   Guidance of Industrial Structure Adjustment in China in 2011, and restricted elimination of PFOA/PFOS substances

45   production were conducted. With a large quantity of PFAAs and their products manufacturing and consumption, China

46   has become the emerging contamination hotspots in the world. In spite of several studies on atmospheric PFAAs levels

47   having been conducted in a few cities (Liu et al., 2015) and point sources (Yao et al., 2016a;Tian et al., 2018) in China,

48   due to the imbalanced urbanization and industrialization levels, there is still a lack of systemic research on atmospheric

49   PFAAs quantification and trends in China.

50   Additionally, the long range or mesoscale transport was also suggested to have a contribution to PFAAs in the air (Dreyer

51   et al., 2009;Cai et al., 2012a). In general, three pathways/hypotheses for the transportation of PFAAs were suggested:

52   transport associated with particles, degradation from precursor, and sea salts from current bursting in coastal areas. The

53   PFAAs precursors such as fluoro–telomere alcohols (FTOHs), which can form the corresponding PFAAs through

54   oxidation reactions initiated by hydroxyl radicals (OH·) in the atmosphere (Thackray and Selin, 2017), are more volatile

55   than PFAAs and can reach remote areas via long–range transportation (Martin et al., 2006; Wang et al., 2018). Due to the

56   lower acid dissociation coefficient (pK_A), 0–3.8 for PFCAs and –3.3 for PFSAs, PFAAs are expected to be mainly

57   associated with aerosols in the non–volatile anionic form (Lai et al., 2018;Pavlína et al., 2018). However, recent field

58   studies have confirmed their occurrence in gaseous phase (Lai et al., 2018;Cassandra et al., 2018;Ahrens et al., 2013).

59   Investigating the transport pathways of PFAAs in nationwide region via active air sampler (AAS) is challenging, due to

60   their electronic power supply and high cost. Fortunately, a number of reports showed that the XAD (a

61   styrene–divinylbenzene copolymer) impregnated sorbent based passive air sampler (SIP–PAS) and XAD based PAS

62   (XAD–PAS), were proven to be an ideal alternative sampling tool for monitoring PFAAs in a wide region, which was

63   suggested to collect a representative sample of both gas and particle phases (Lai et al., 2018;Pavlína et al., 2018).

64   XAD–PAS give PFASs profiles that were more closely resembled to those from AAS in comparing with PUF–PAS, have

65   sufficient uptake rates for the PFCAs and PFSAs to be depoyled for short time duration (Lai et al., 2018).

66   Given the factors mentioned above, we conducted a nationwide survey of PFAAs in China at a provincial level using a

67   XAD–PAS from January to December in 2017. The objective of this research was: (1) to examine the tempo–spatial

68   variations of PFAAs, and (2) to identify their potential affecting factors and evaluate the affecting pathways. To the best

69   of our knowledge, this is the first research paper analyzing both a long–term and nationwide atmospheric PFAAs data set

70   complemented by a comprehensive investigation in China.

71   **2.Material and methods**

72   **2.1 Chemicals and reagents**

73   The PFAAs standards used were Wellington Laboratories (Guelph, ON, Canada) PFAC–MXB standard materials,

74   including C5–C14 PFCAs analogues (PFPeA, PFHxA, PFHpA, PFOA, PFNA, PFDA, PFUdA, PFDoA, PFTrDA,

75   PFTeDA, and PFHxDA), as well as C4, C6, and C8 PFSAs analogues (PFBS, PFHxS, and PFOS). The mass–labeled

76    $1,2–^{13}C_2$–PFHxA, $1,2,3,4–^{13}C_4$–PFOA, $1,2,3,4,5–^{13}C_5$–PFNA, $1,2–^{13}C_2$–PFDA, $1,2–^{13}C_2$–PFUdA, $1,2–^{13}C_2$–PFDoA,

77    $^{18}O_2$–PFHxS, and $1,2,3,4–^{13}C_4$–PFOS were used as internal standards (ISs, MPFAC–MXA, Wellington Laboratories Inc.)

78   in high–performance liquid chromatography (HPLC) coupled with a tandem mass spectrometer (MS/MS). HPLC–grade

79   reagents that were used include methanol, ethyl acetate, ammonia acetate, acetone, methylene dichloride, n–hexane, and

80   Milli–Q water. Detailed sources of the target PFAAs and their ISs are listed in Table S1 in the Supplementary Materials.

81   **2.2 Sample collection**

82   Sampling campaigns were carried out at 23 different provinces/municipalities/autonomous regions in China

83   simultaneously from January to December 2017, of which 20 were urban sites and three were rural sites (Zhejiang,

84   Shanxi, and Liaoning). Urban samples typically came from urban residential areas, and the rural samples were obtained

85   from villages. These sampling sites were divided into seven administrative divisions: norther of China (NC), southern of

86   China (SC), central of China (CC), eastern of China (EC), northwest of China (NW), northeast of China (NE), and

Atmospheric
Chemistry
and Physics
Discussions

87   southwest of China (SW). A geographical map of the sampling sites is displayed in Figure S1, and the detailed

88   information on sampling sites such as elevation , meteorological parameters, local resident population and gross domestic

89   product were listed in Table S2.

90   Samples were collected with Amberlite XAD–2 resin using XAD–PAS, which have been successfully monitored PFCAs

91   (C4–C16) and PFSAs (C4–C10) in the atmosphere (Krogseth et al., 2013;Armitage et al., 2013). Briefly, the mesh

92   cylinder (L.× I.D.: 10 cm × 2 cm) was prebaked at 450°C for 3 h, filled with ~10 g XAD–2 resin, and capped with an

93   aluminum cap. The sampling program for each sample lasted approximately a month (30 days), and the error of the

94   sampling time was controlled within 3 d. At the end of each deployment period, the atmosphere samples were retrieved,

95   resealed in their original solvent–cleaned aluminum tins at the sampling location, and transported by express post to

96   Shanghai Jiao Tong University. On receipt, they were stored and frozen (–20°C) until extraction.

97   The sampling rate of XAD–PAS is a crucial factor to derive the chemical concentrations accumulated in the XAD resin.

98   Ahrens et al. (2013) found that sampling rate of PFCAs and PFASs ranged 1.8–5.5 m^3/d with XAD impregnated sorbent,

99   and the sampling rate increased as the carbon chain adding, while Karásková et al. (2018) suggested that the sampling

100   rate of XAD–PAS of 0.21–15 m^3/d for PFAAs. The loss of depuration compounds could be used to calculate the

101   sampling rate, assessing the impacts from meteorological factors like temperature and wind speed. According to Ahrens

102   et al. (2013) the 1,2,3,4–$^{13}C_4$–PFOA was used to calculate the sampling rates of PFAAs at Shanghai sampling site

103   (Shanghai Jiao Tong University) in the present study, by assessing 1,2,3,4–$^{13}C_4$–PFOA abundance loss. The specific

104   description of the sampling rate calculation in this study is shown in Section S1 in the Supplementary Materials.

105   **2.3 Sample preparation and instrument analysis**

106   The sample preparation and analysis were according to the method described by previous researches (Liu et al.,

107   2015;Tian et al., 2018). The MPFAC–MXA ISs mixture surrogates (10 ng) were added to each spiked sample prior to

108   extraction. This was done to account for the loss of substances from the samples associated with instrument instability

109   caused by the changes in laboratory environmental conditions. The XAD resin samples were Soxhlet–extracted for 24 h

110   using a Soxhlet extraction system, with n–hexane: acetone (1:1, V:V) as a solvent in a 300 mL polypropylene (PP) bottle,

111   following extracted with methanol for 4 h. These two extracts were combined and reduced to ~5 mL via a rotary

112   evaporator (RE–52AA, Yarong Biochemical Instrument Inc., Shanghai, China) at a temperature below 35°C, and then

113   transferred to a 10 mL PP tube for centrifugation (10 min, 8,000 rpm). The supernatant was transferred to another PP tube,

114   filtered three times through a 0.22 μm nylon filter, with an addition of 1 mL methanol each time. The extracts were

115   further condensed under a gentle stream of nitrogen (99.999%, Shanghai Liquid Gas Cor.) at 35°C to a final 200 μL for

116   instrument analysis.

117   The separation and detection of PFAAs were performed using a HPLC system (Thermo Ultra 3000[+], Thermo Scientific,

118   USA) coupled with a triple quadrupole negative electrospray ionization MS/MS (Thermo API 3000, Thermo Scientific,

119   USA). An Agilent Eclipse XDB C18 (3.5 μm, 2.1 mm, 150 mm) was used to separate the desorbed substances. The

120   column temperature was set to 40ºC, and the flow rate was 0.30 mL/min. The injection volume was 20 μL. The gradient

121   elution program of the mobile phase A (methanol) and B (5 mmol/L aqueous ammonium acetate) was 20% A + 80% B at

122   the start, 95% A + 5% B at 8 min, 100% a at 13 min, 20% A + 80% B at 14 min, and was maintained for 6 min. The

123   MS/MS was operated in a negative ion scan and multiple reaction monitoring (MRM) mode, and the electrospray voltage

124   was set to 4500 V. The ion source temperature was 450ºC. The flow rates of the atomization gas and air curtain gas was

125   10 and 9 L/min, respectively. Species identification was achieved by comparing the mass spectra and retention time of

126   the chromatographic peaks with the corresponding authentic standards.

127   **2.4 Quality assurance and quality control**

128   To avoid exogenous contamination, the XAD–2 resin was precleaned using a Soxhlet extraction system with acetone and

129   petroleum ether at extraction times of 24 h and 4 h, respectively. The extracted XAD resin was dried under a vacuum

130   desiccator, wrapped in an aluminum foil and zip–lock bags, and stored at –20°C to avoid contamination. All laboratory

131   vessels were PP, and these vessels were washed with ultrapure water and methanol three times, respectively.

132   For quantification, six–point calibration curves of PFAAs were constructed by adopting different calibration solutions

133   with values of 1, 3, 6, 15, 30, and 60 ng/mL. The same concentration for the internal calibration (10 ng/mL) was used for

134   each level of the calibration solution. Recovery standards were added to each of the samples to monitor procedural

135   performance, and the mean spiked PFAAs recoveries ranged from 81%±25% to 108%±22%. All the analyzed PFAAs

136   were normalized against the recovery of the corresponding mass–labeled ISs. Field blanks were prepared at all sampling

137   sites, transported, and analyzed in the same way as the samples. Laboratory blanks were obtained by taking amounts of

138   solvent via extraction, cleanup, and analysis. A total of 8 field blanks and 26 laboratory blanks were analyzed, and all the

139   results were corrected according to the blank and recovery results. The method detection limit (MDL) was derived from

140   three times standard deviation of the field blank values. The limit of detection (LOD) and the limit of quantification

141   (LOQ) were determined as a signal–to–noise ratio of 3:1 and 10:1, respectively (Rauert et al., 2018;Liu et al., 2015). To

142   convert MDLs, LODs and LOQs values to pg/m^3, the mean volume of sampling air (m^3) was applied. For the analytes

143   that were not detected or were below the LOQs in field blanks, MDLs were derived directly from three times the

144   corresponding LODs. More detailed information on the individual compounds of PFASs on MDL, LOD, LOQ, and the

Atmospheric
Chemistry
and Physics
Discussions

145   recovery values are listed in Table S3.

2.5 Statistical and geostatistical analysis

147   Statistical analyses were carried out by SPSS Statistics 22 (IBM Inc. US) and SigmaPlot 14.0 (Systat Software, US). And

148   the geographical variations of atmospheric PFAAs were analyzed with ArcGIS 10.4 (ESRI, US). Positive matrix

149   factorization (PMF) is considered an advanced algorithm among various receptor models, which has been successfully

150   applied for source identification of environmental pollutants (Han et al., 2018;Han et al., 2019) . PMF (5.0, US EPA) was

151   adopted to cluster the PFAAs with similar behaviors to identify potential sources, and a more detailed description of PMF

152   can be seen in Section S2.

3.Results and discussion

3.1 Abundances and compositions

155   The descriptive statistics of all targeted atmosphere PFAAs (n=268) are presented in Table 1 and Table S4. The total

156   concentrations of Σ_{13} PFAAs analogues varied between 6.19 and 292.6 pg/m^3, with an average value of 39.8±28.1 pg/m^3.

157   The commonly concerned PFCAs analogues (C5–C14) occupied 79.6% of the total PFAAs, at a level of 4.50–247.2

158   pg/m^3, whereas the PFSAs concentrations were 1.04–42.6 pg/m^3. The long–chain PFCAs concentrations were 25.6±18.9

159   pg/m^3, which were significantly higher than the short–chain (C $\leq$ 6) concentrations (12.3±10.9 pg/m^3) (p<0.05). To the

160   contrary, a recent measurement found the long chain (C $\geq$ 8) PFCAs were much higher which conducted in the landfill

161   atmosphere in Tianjin, China (Tian et al., 2018). Specifically, PFOA was the dominant PFAAs (accounting 20.6%), and

162   was detected in all atmospheric samples with an average value of 8.19±8.03 pg/m^3. This phenomenon could occur since

163   PFOA is widely used in the manufacturing of polytetrafluoroethylene (PTFE), perfluorinated ethylene propolymer (FEP),

164   and perfluoroalkoxy polymers (PFA) (Wang et al., 2014). The domestic demand for and the industrial production of

165   PFOA–based products have been increasing in China since the late 1990s (Wang et al., 2014), and direct emissions of

166   FOSA–based products may contribute to the relative high level of PFOA. Meanwhile, one major variation of PFOA

167   precursor, 8:2 FTOH, was reported ranks as the highest concentration among neural PFASs in China air (De Silva,

168   2004;Martin et al., 2006). Among PFAAs' composition profile, it was followed by PFHxA, PFOS, and PFPeA, with

169   mean concentrations of 5.36, 5.20, and 4.95 pg/m^3, respectively. The detection frequencies of PFCAs decreased gradually

170   as the carbon chain length increased – for instance, the PFPeA and PFTrDA were detected in 84.8% and 37.3%,

171   respectively.

172   Compared with other gaseous PFAAs measurements, Liu et al. (2015) reported that PFAAs in the urban atmosphere

173 sampled with XAD–containing sorbent in Shenzhen city in China was 15±8.8 pg/m^3, which contributed to nearly half of

174 this study. Wong et al. (2018) found that a much lower PFAAs levels in the remote Arctic area than this study, with mean

175 value of 1.95 pg/m^3. This study found generally higher PFAAs abundances compared to measurement in Canada

176 (Gewurtz et al., 2013), which may be attributed to the relative high abundance of industrial and domestic emissions in

177 China. However, the PFAAs concentrations in urban/rural areas in this study were far lower than the measurements at

178 point sources, for example, landfill atmosphere (Tian et al., 2018) (360–820 pg/m^3) and fluorochemical manufacturing

179 facility (Chen et al., 2018) (4900±4200 pg/m^3), suggesting that PFAAs were susceptible to being affected by local source

180 emissions.

181

182 **Table 1.** Comparison of PFAAs levels in the present research with measurements in other areas (pg/m^3)

Sampling sites	Duration	Sampling location	Sampler type [a]	PFAAs [b]	PFCAs [c]	Reference
23 provinces in China	2017.1–12	Urban and rural areas	XAD–PAS	6.19–292.6; 39.8±28.1	4.50–247.2; 31.7±23.9; C5–C14	This study
Shenzhen, China	2011.9–11	Urban area	SIP–PAS	3.4–34; 15±8.8	11.59±8.74; C4–C12	(Liu et al., 2015)
Fuxin, China	2016.9–10	Fluorochemical manufacturing facilities	SIP–PAS	4900±4200	4900±4200; C4–C12	(Chen et al., 2018)
Tianjin, China	2013	Waste water treatment plant	SIP–PAS	87.9–227; 123	87.9–227; 123; C6–C12	(Yao et al., 2016a)
Tianjin, China	2016.5–6	Landfill	SIP–PAS	280–820	280–820; C4–C12	(Tian et al., 2018)
Canada	2006–2011	Remote and urban areas	SIP–PAS	0.014–0.44	0.014–0.44; C8–C12	(Gewurtz et al., 2013)
Alert, Arctic	2006.8–2015.2	Remote area	SIP–PAS	1.95	1.95; C4–C8	(Wong et al., 2018)
Toronto, Canada	2010.3–10	Semi–urban site	XAD–PAS	0.7–20	0.7-20; C4–C15	(Ahrens et al., 2013)
Brno, Czech Republic	2013.4-9	Suburban background site	SIP–PAS	30–153	26–147.6; C4–C14	(Pavlína et al., 2018)

183 [a]: SIP-PAS represent XAD impregnated sorbent based PAS;

184 [b]: represent concentration range; mean value;

185 [c]: represent concentration range; mean value; carbon length of PFCAs.

186   **3.2 Temporal variations**

187   Monthly and seasonal variations of the mean PFAAs concentrations are depicted in Figure 1. In general, an increasing

188   seasonal mean of PFAAs concentrations existed for summer (31.4 pg/m^3) < autumn (35.6 pg/m^3) < spring (42.4 pg/m^3) <

189   winter (52.8 pg/m^3). The winter maxima abundance of PFAAs may be could attribute to the stagnant atmospheric

190   conditions, in which atmospheric contaminants were trapped in the air with a weak diluting effect. XAD–PAS showed

191   similar efficiency of capturing gas and particle phases PFASs, while the unimpeded particle gathering efficiency is

192   challenging to quantify. In addition, despite the increase in atmospheric oxidation of precursors in summer may lead to

193   PFCAs rise (Li et al., 2011;Yao et al., 2016a), the abundant rainfall would enhance their scavenging activities (Table S5),

194   ultimately leading to the relatively low concentrations of PFAAs in the summer. Specifically, the PFAAs showed much

195   higher concentrations in spring than other seasons in Shanghai, which was different from Tianjin and Xinjiang (Figure

196   S2). An extreme high level of PFAAs of 135.5 pg/m^3 was occurred in November in Beijing, which was 2–4.5 times

197   higher than in other month, indicating the potential point source of PFAAs contamination in this site. In fact, numerous

198   fluoride related products manufacturers were distributed in EC, NC (including Beijing) and CC areas, see detail in Figure

199   S3. As gaseous PFAAs measurements were majorly reported at a relative short time (several weeks to several months), it

200   is somewhat difficult to compare their temporal trends.

201   Interestingly, the evolution of PFAAs showed a dramatic monthly variation, and the monthly mean levels varied from

202   25.9 to 60.6 pg/m^3, with the lowest and the highest abundances being present in September and December, respectively.

203   For the specific composition profile of PFAAs, the average concentrations of PFOA, PFHxA, PFPeA, and PFOS were

204   10.4, 8.42, 6.55, and 6.44 pg/m^3 in winter, respectively, which were nearly two times higher than in the summer. The

205   seasonal variation trend of PFOS was summer < spring ≈ autumn < winter, while PFNA appeared to show winter maxima

206   with concentrations 4 and 3 times higher than in the summer and spring, respectively. However, Wong et al. (2018)

207   reported that PFBS showed the maximal value in winter but found no consistent seasonality for PFOS in the Arctic area.

208   The differences may be explained as the PFAAs in air in the remote Arctic area were originated from long–range

209   transport and volatilization from snow or sea, but not affected by local direct anthropogenic emission.
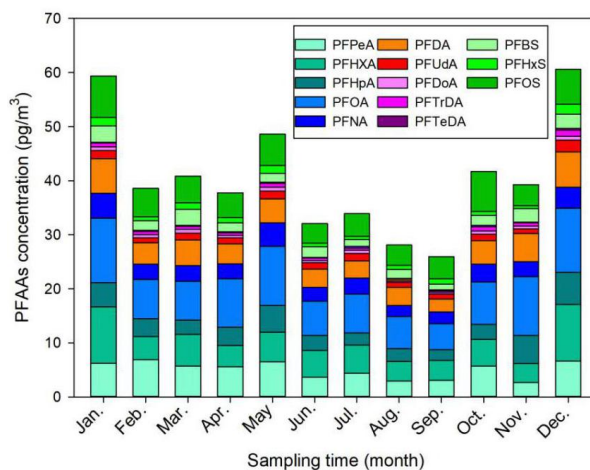
Fig. 1. Monthly mean concentrations of PFAAs in China from January to December 2017

3.3 Geographical distributions

Due to the stark differences in topography and socioeconomic development of Chinese provinces, municipalities, or autonomous regions, as well as the enormous differences in industrialization and emissions, PFAAs showed significantly different distribution patterns in China (Figure 2). Overall, the predominant declining gradient of PFAAs' contents was CC> NC> EC> NE> SW> NW> SC areas in China, which was similar to previous research that the outdoor dust–bounded PFAAs were relatively enriched in the eastern part of mainland China (Yao et al., 2016b). This trend was not surprising since numerous PFAAs related photoelectric industries, chemical industries, and mechanical industries are dispersed across CC, EC and NC areas, e.g., Shanghai, Zhejiang, Fujian, Henan, and Jiangsu. As expected, the western mountain and highland areas, e.g., Xinjiang and Yunnan (20.9 pg/m^3), with relatively low population densities and high latitudes, displayed significantly lower PFAAs concentrations. It was reported that high orographic conditions have a cold trapping effect on atmospheric PFASs, the transportation of PFAAs involving particles or not should be dramatically reduced (Konstantinos et al., 2010;Yao et al., 2016a). Given that altitudes increase gradually from several meters in EC, NC and SC coastal areas to nearly 2,000 meters in SW and NW highland regions in China, the high altitude blocking effect for atmospheric PFAAs transportation should not be neglected.

The annual average concentrations of PFAAs at the provincial level ranged from 12.4 pg/m^3 in Xinjiang to 90.9 pg/m^3 in Henan, and the composition patterns varied widely. Henan contributed the largest proportion of PFAAs in China, and showed the highest PFOA level (19.1 pg/m^3), which is a typical, heavily–industrialized province characterized by textile

230   treatments, metal plating, and firefighting foam manufacturing, and a large amount of PFAAs emulsifier fluoropolymers

231   were used in industrial production. Special attention should be paid to Zhejiang, the level of which (61.7 pg/m^3) ranked

232   second in PFAAs abundances in spite of its sampling site being located in a village. As well as this, several

233   painting–packaging plants, mechanical plants, and electrical equipment manufacturers were dispersed around this

234   sampling site (see Figure S4), which would contribute to the PFAAs variations in this site. In fact, the GDP of Zhejiang

235   ranked fourth in China, specializing in mechanical manufacture, textiles, and chemical industry. Moreover, the top six

236   sites with abundant of PFAAs were located in the most economically–developed and populated areas (the Yangtze River

237   Delta area, the Circum–Bohai Sea Region), and in the rapidly–developing regions (Henan, Sichuan) in China. In line

238   with this result, a sampling campaign conducted in Asia, including 18 sites in China, found very high levels of PFAAs

239   precursors (8:2 FTOH, 10:2 FTOH) existed in Beijing, Tianjin, and Zhejiang (Li et al., 2011). But meanwhile we should

240   keep in mind that the production of PFCAs in the atmosphere from gaseous precursors degradation may be impaired in

241   urban areas, due to the high abundance of NOx compete for OH· radicals.

242   Furthermore, PFOA concentrations were apparently high in Henan, Zhejiang, Beijing, Tianjin, and Hubei, where mean

243   values ranged of 11.7–19.1 pg/m^3 compared with in other provinces (2.93–8.54 pg/m^3). PFOA and PFOA–related

244   products have not been banned for use in various industrial and domestic applications (Konstantinos et al., 2010;Wang et

245   al., 2014), which were manufactured extensively in EC and NC areas and were used widely. However, the highest

246   concentration of PFOS was found in Zhejiang (14.1 pg/m^3), which may be affected by local manufacturing of PFOS

247   based products, e.g. leather, paper and metal plating. It was followed by Beijing (8.98 pg/m^3) and Fujian (9.09 pg/m^3),

248   while Xinjiang and Yunnan shared the lowest levels (1.20–3.57 pg/m^3). This spatial variation patterns of PFOS in the

249   present study, matched well with a previous national survey that found most PFOS and its derivative facilities in China

250   are suited in EC, CC and NC areas, with emission density ranged from 1–500 g/(km^2·a) (Konstantinos et al., 2010;Wang
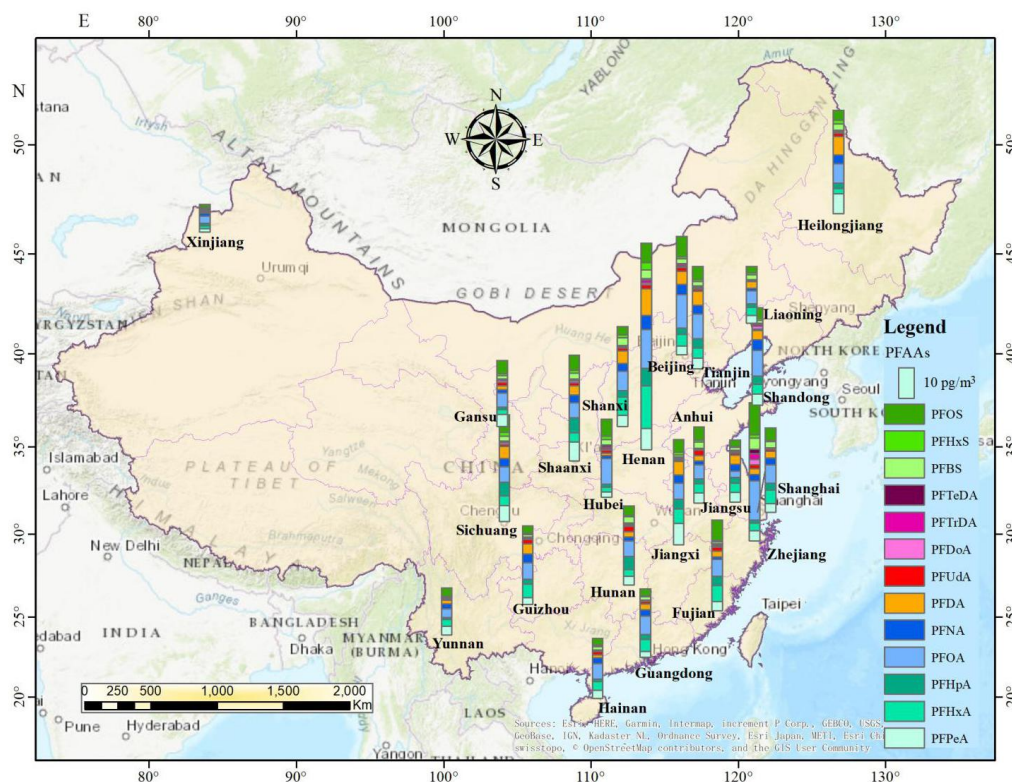
251   et al., 2014).

Fig. 2. The spatial distributions of PFAAs in China (annual average of PFAAs, created by ArcGIS 10.4).

3.4 Geographical distributions transport pathway

The PFAAs variations in the atmosphere depended on their local source emissions as well as regional atmosphere transportation. In order to give readers a direct impression of factors affecting the geographical variations of PFAAs in China, here we analyzed PFAAs variations along three pathway transects and one coastal line to determine how PFAAs distribute spatially.

As shown in Figure 3a, PFAAs concentrations were enriched in southeastern areas (40.6–47.2 pg/m^3) at low altitudes (2–30 m), but relatively low abundances (12.3–29.4 pg/m^3) existed in the northwestern part of China (397–1,517 m in altitude). As discussed above, the EC areas (e.g. Fujian) were the most intensively industrialized regions, direct emissions from PFAAs manufacturing processes would enhance their atmospheric abundances. However, high altitudes existed in NW areas would have a blocking effect to the transportation of PFAAs from eastern polluted areas.

In terms of the SW–NE transect (Figure 3b), Yunan and Liaoning showed much lower PFAAs concentrations (20.9 and

266   25.0 pg/m^3) than other areas (44.8–52.6 pg/m^3). Notably, a steady increasing trend of PFAAs concentrations existed

267   across the W–E transect (Figure 3c), which escalated from 20.9 pg/m^3 in Yunnan to 61.7 pg/m^3 in Zhejiang. The

268   composition profiles of PFAAs along this transect differed from each other; for instance, PFOA occupied 28.5% of the

269   total PFAAs in Zhejiang, while it only accounted for 15.6%–21.8% in other areas. Note that PFAAs released from point

270   sources would be eliminated by deposition, degradation, or dilution during transportation in the atmosphere, e.g., PFOA

271   could decrease by 90% within 5 km of its point source (Chen et al., 2018). However, the long range transport of PFAAs

272   bounded with particles also have been explored in previous research (Pickard et al., 2018), our Hysplit back–trajectories

273   analysis results for Zhejiang, Jiangxi, and Shanghai confirmed that the air mass origins was a driving factor for PFAAs

274   variation(see Figure S5).

275   Interestingly, with the exclusion of the site directly affected by surrounding sources in Zhejiang, PFAAs were rather

276   uniformly distributed among the coastal areas, with concentrations ranging from 24.9–45.8 pg/m^3 (Figure 3d). Excluded

277   industrial and domestic emissions as well as secondary formation, the PFAAs containing sea spray aerosols could

278   contribute the variations of PFAAs in coastal atmosphere (Cai et al., 2012b; Pickard et al., 2018).
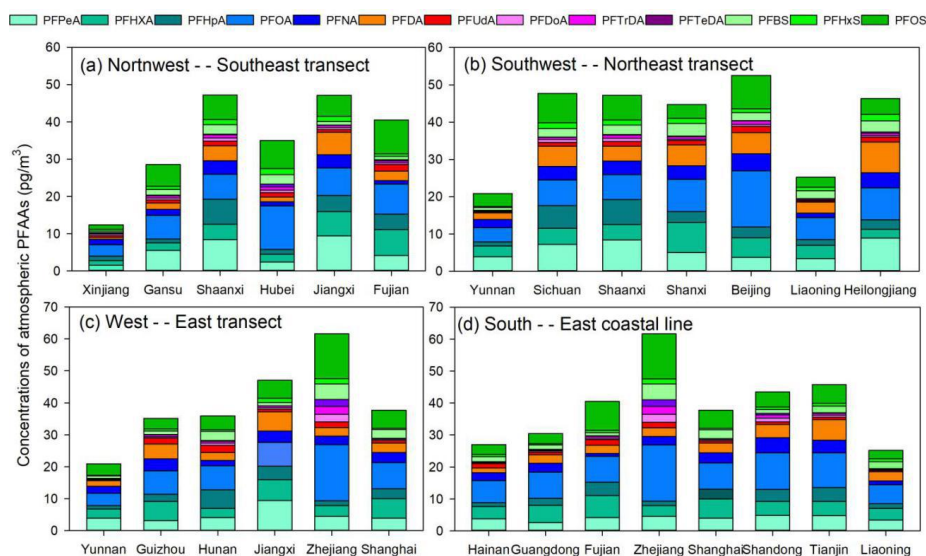
279

280   **Fig. 3.** Transects of PFAAs concentrations across three different directions and one coastal line

281

282   **3.5 Source identification**

283   Understanding the sources of PFAAs and their corresponding importance would enable elucidation of the levels of

284   PFAAs in the environment. As discussed above, the observations from tempo–spatial variations of PFAAs suggest that

Atmospheric
Chemistry
and Physics
Discussions

285   several factors may have a combined effect on the variations of PFAAs. Hence, a PMF model was adopted to extract the

286   potential factors affecting PFAAs variations, and four sources were extracted in this study (see Figure 4).

287   High percentages (~90%) of PFPeA and PFBS were found in factor 1, and were moderately loaded with PFOS (62.6%).

288   Three major types of PFOS–related chemicals; namely PFOS salts, PFOS substances and PFOS polymers, are used in

289   industrial products in China (Xie et al., 2013). PFOS salts are usually used in metal plating, firefighting foams, and

290   pesticides, while PFOS substances are adopted in paper treatment and the semiconductor industry. PFOS polymers are

291   employed for textile and leather treatment. These PFOS–related products would lead to direct emissions of PFOS during

292   their industrial and domestic activities. PFPeA and PFBS are the main substitutes for long–chain PFAAs in China, which

293   would release as impurities or by–products when manufacturing PFOS–based products (Liu et al., 2017). Hence, this

294   factor was regarded as the direct source of PFOS–based products. This was consistent with the spatial observations that

295   high PFOS concentrations were shown in Zhejiang, Fujian, Guangdong, and Shanghai, where manufacturing facilities are

296   distributed.

297   Factor 2 was characterized by PFHxA, PFOA, PFNA, and PFDA, each representing over 60% of their explained

298   variations. Their rather strong positive correlations ($r=0.54$–0.84, $p<0.01$) suggested that they may have originated from a

299   similar source (Table S6). PFOA was considered as the marker for the emulsification of plastics, rubber products, flame

300   retardants for textiles, paper surface treatments and fire foams (Liu et al., 2015;Konstantinos et al., 2010). It has been

301   reported that there was an increase in PFCAs emissions at the manufacturing sites of PFOA–based products in China

302   between 2002 and 2012 due to a rapid increase in domestic demand and production of PFOA–related products (Wang et

303   al., 2014). PFNA and its derivatives have similar physicochemical properties to PFOA and its derivatives, and both can

304   be emitted through exhaust gases. The PFNA–based production was found to be related to polyvinylidene fluoride

305   (PVDF) production, and it has been suggested that PVDF production increased in China after 2008 (Wang et al., 2014).

306   Therefore, factor 2 represents direct sources of PFOA–based and PFNA–based products.

307   The compositions of factor 3 were characterized by a high loading of PFHpA and PFHxS, with loading factor values of

308   84.9% and 81.7%, respectively. The historical production and uses of PFHpA and its derivatives remain unidentified.

309   Factor with PFHxS alone did not indicate a specific source, so this factor may be classified as an unknown source, which

310   may be affected by atmosphere air mass transport, sea aerosol bursting and/or other origins.

311   The final factor was dominated by PFUdA, PFDoA, PFTrDA, and PFTeDA, with loading factor values larger than 80%.

312   These long–chain PFAAs (C11–C14) analogues have been interpreted as degradation products of fluorotelomer–based

313   products in previous research (Liu et al., 2017;Wang et al., 2014; Thackray and Selin, 2017). Based on the life–cycle

314   usage and release from fluorotelomer and other fluorinated products, the global cumulative estimation of PFUdA,

Atmospheric
Chemistry
and Physics
Discussions

315   PFDoA, PFTrDA, and PFTeDA from quantified sources was estimated to be 9–230 tons in the period of 2003–2015, and

316   projected to be between 0–84 tons between 2016–2030 (Wang et al., 2014). It was reported that the manufacturing of

317   fluorotelomer–based substances would increase in China. In addition, these four analogues showed apparent positive

318   correlations each other (r =0.59–0.79, p<0.01). Thus, this factor was explained as the degradation products of

319   fluorotelomer–based products, which could be proven by their higher abundances caused by an enhanced atmospheric

320   oxidation ability in the summer than other seasons.

321   Direct emission sources, including PFOS–based products, PFOA–based products, and PFNA–based products were

322   estimated to represent 62.7% of the total PFAAs sources. Indirect sources of degradation products of

323   fluorotelomer–based products played a minor role, contributing 15.5%, and there are 21.8% of variances that could still

324   not be explained and need further detailed investigation. This source apportionment result was similar to one recent piece

325   of research that found that industrial PFOA emissions were the major sources of atmospheric PFAAs in Shenzhen, China

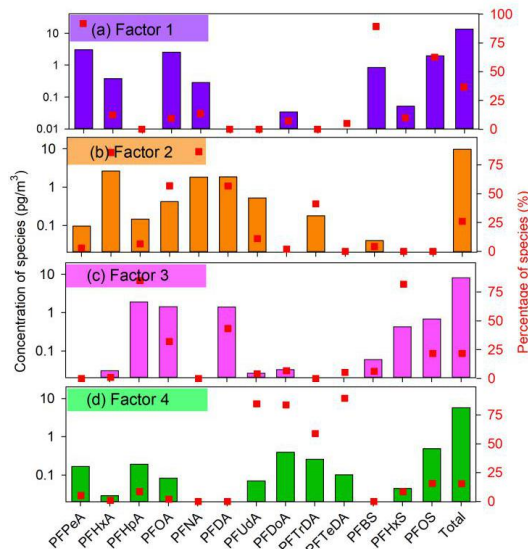326   (Liu et al., 2015), and the long–distance transportation of pollutants also made a contribution.

327

328   **Fig. 4.** Factor profiles of PFAAs extracted by the PMF model

329   **4. Conclusion**

330   In the present study, PFAAs were ubiquitously detected in the atmosphere across China over the length of a year. Results

331   indicated that the measured PFAAs were several times to several magnitudes higher than other urban atmosphere levels,

332   and much higher abundances existed in winter seasons compared with in the summer. In terms of spatial distribution, the

333 PFAAs concentrations were higher in central and eastern China, where dense residential and industrial manufacturing

334 facilities were distributed. Correlation, Hysplit backward trajectories, and a PMF receptor model suggested that the direct

335 sources of PFOS–based, PFOA–based, and PFNA–based products made a predominant contribution to variations in

336 PFAAs, while indirect degradation played a minor role.

Acknowledgements

Appendix A: Supplementary material

References

347 Ahrens, L., Harner, T., Shoeib, M., Koblizkova, M., and Reiner, E. J.: Characterization of Two Passive Air Samplers for

348 Per- and Polyfluoroalkyl Substances, Environ. Sci. Technol., 47, 14024-14033, https://doi.org/10.1021/es4048945, 2013.

349 Armitage, J. M., Hayward, S. J., and Frank, W.: Modeling the Uptake of Neutral Organic Chemicals on XAD Passive Air

350 Samplers under Variable Temperatures, External Wind Speeds and Ambient Air Concentrations (PAS-SIM), Environ. Sci.

351 Technol., 47, 13546-13554, https://doi.org/10.1021/es402978a, 2013.

352 Baard Ingegerdsson, F., Line Sm. Stuen, H., Raymond, O., Hanne Line, D., Merete, H., Cathrine, T., Syvert, T., Georg, B.,

353 Paal, M., and Ellingsen, D. G.: Occupational exposure to airborne perfluorinated compounds during professional ski

354 waxing, Environ. Sci. Technol., 44, 7723-7728, https://doi.org/10.1021/es102033k, 2010.

355 Cai, M., Xie, Z., Moeller, A., Yin, Z., Huang, P., Cai, M., Cai M. Yang, H., Sturm, R., and He, J.: Polyfluorinated

356 compounds in the atmosphere along a cruise pathway from the Japan Sea to the Arctic Ocean, Chemosphere, 87(9),

357 989-997 https://doi.org/ 10.1016/j.chemosphere.2011.11.010, 2012a.

358 Cai M., Zheo, Z., Yin Z., Ahrens L., Huang P., Cai M., Yang H., He J., Sturm R., Ebinghaus R., Xie Z.: Occurrence of

359   perfluoroalkyl compounds in surface waters from the North Pacific to the Arctic Ocean, Environ. Sci. Technol., 46,

360   661-668, https://doi.org/10.1021/es2026278, 2012b.

361   Cassandra, R., Tom, H., K, S. J., Anita, E., Gilberto, F., Eugenia, C. L., Oscar, F., Martin, V. I., S.B., M. K., and Isabel, M.

362   R.: Atmospheric concentrations of new POPs and emerging chemicals of concern in the Group of Latin America and

363   Caribbean (GRULAC) region, Environ. Sci. Technol., 52(13), 7240-7249, https://doi.org/10.1021/acs.est.8b00995, 2018.

364   Chen, H., Yao, Y., Zhao, Z., Wang, Y., Wang, Q., Ren, C., Wang, B., Sun, H., Alder, A. C., and Kannan, K.: Multimedia

365   Distribution and Transfer of Per- and Polyfluoroalkyl Substances (PFASs) Surrounding Two Fluorochemical

366   Manufacturing Facilities in Fuxin, China, Environ. Sci. Technol., 52, 8263-8271, https://doi.org/10.1021/acs.est.8b00544,

367   2018.

368   De Silva, A. O.: Degradation of fluorotelomer alcohols: a likely atmospheric source of perfluorinated carboxylic acids,

369   Environ. Sci. Technol., 38, 3316-33121, https://doi.org/10.1021/es049860w, 2004.

370   Dreyer, A., Weinberg, I., Temme, C., and Ebinghaus, R.: Polyfluorinated Compounds in the Atmosphere of the Atlantic

371   and Southern Oceans: Evidence for a Global Distribution, Environ. Sci. Technol., 43, 6507-6514, https://doi.org/

372   10.1021/es9010465, 2009.

373   Gewurtz, S. B., Backus, S. M., Silva, A. O., De, Lutz, A., Alain, A., Marlene, E., Susan, F., Melissa, G., Paula, G., and

374   Tom, H.: Perfluoroalkyl acids in the Canadian environment: multi-media assessment of current status and trends, Environ.

375   Int., 59, 183-200, https://doi.org/10.1016/j.envint.2013.05.008, 2013.

376   Han, D., Fu, Q., Gao, S., Li, L., Ma, Y., Qiao, L., Xu, H., Liang, S., Cheng, P., Chen, X., Zhou, Y., Yu, J. Z., and Cheng,

377   J.: Non-polar organic compounds in autumn and winter aerosols in a typical city of eastern China: size distribution and

378   impact of gas–particle partitioning on PM2.5 source apportionment, Atmos. Chem. Phys., 18, 9375-9391, https://doi.org/

379   10.5194/acp-18-9375-2018, 2018.

380   Han, D., Fu, Q., Gao, S., Zhang, X., Feng, J., Chen, X., Huang, X., Liao, H., Cheng, J., and Wang, W.: Investigate the

381   impact of local iron–steel industrial emission on atmospheric mercury concentration in Yangtze River Delta, China,

382   Environ. Sci. Pollut. Res., 26(6), 5862–5872, https://doi.org/10.1007/s11356-018-3978-7, 2019.

383   Hu, X. C., Andrews, D. Q., and Lindstrom, A. B.: Detection of Poly- and Perfluoroalkyl Substances (PFASs)in U.S.

384   Drinking Water Linked to Industrial Sites, Military Fire TrainingAreas, and Wastewater Treatment Plants, Environ. Sci.

385   Technol. Lett., 3, 344-350, https://doi.org/10.1021/acs.estlett.6b00260, 2016.

386   Jian, J. M., Guo, Y., Zeng, L., Liu, L. Y., Lu, X., Wang, F., and Zeng, E. Y.: Global distribution of perfluorochemicals

387   (PFCs) in potential human exposure source–A review, Environ. Int., 108, 51-62, https://doi.org/ , 2017.

388   Johansson, N., Fredriksson, A., and Eriksson, P.: Neonatal exposure to perfluorooctane sulfonate (PFOS) and

389   perfluorooctanoic acid (PFOA) causes neurobehavioural defects in adult mice, Neurotoxicology, 29, 160-169,

390   https://doi.org/10.1016/j.neuro.2007.10.008, 2008.

391   Karásková, P., Codling, G., Melymuk, L., and Klánová, J.: A critical assessment of passive air samplers for per- and

392   polyfluoroalkyl substances, Atmos. Environ., 185, 186-195, https://doi.org/10.1016/j.atmosenv.2018.05.030, 2018.

393   Konstantinos, P., Cousins, I. T., Buck, R. C., and Korzeniowski, S. H.: Sources, fate and transport of

394   perfluorocarboxylates, Environ. Sci. Technol., 40(1), 32-44, https://doi.org/10.1002/chin.200611255, 2010.

395   Krogseth, I. S., Xianming, Z., Ying, D., Lei, Frank, W., and Knut, B.: Calibration and application of a passive air sampler

396   (XAD-PAS) for volatile methyl siloxanes, Environ. Sci. Technol., 47, 4463-4470, https://doi.org/10.1021/es400427h,

397   2013.

398   Lai, F. Y., Rauert, C., Gobelius, L., and Ahrens, L.: A critical review on passive sampling in air and water for per- and

399   polyfluoroalkyl substances (PFASs), TrAC Trends Anal. Chem., Available online 23 Nov. 2018, https://doi.org/

400   10.1016/j.trac.2018.11.009, 2018.

401   Li, J., Vento, S. D., Schuster, J., Gan, Z., Chakraborty, P., Kobara, Y., and Jones, K. C.: Perfluorinated Compounds in the

402   Asian Atmosphere, Environ. Sci. Technol., 45, 7241-7428, https://doi.org/10.1021/es201739t, 2011.

403   Lindstrom, A. B., Strynar, M. J., and Libelo, E. L.: Polyfluorinated Compounds: Past, Present, and Future, Environ. Sci.

404   Technol., 45, 7954-7961, https://doi.org/10.1021/es2011622, 2011.

405   Liu, B., Zhang, H., Yao, D., Li, J., Xie, L., Wang, X., Wang, Y., Liu, G., and Yang, B.: Perfluorinated compounds (PFCs)

406   in the atmosphere of Shenzhen, China: Spatial distribution, sources and health risk assessment, Chemosphere, 138,

407   511-518, https://doi.org/10.1016/j.chemosphere.2015.07.012, 2015.

408   Liu, Z., Lu, Y., Wang, P., Wang, T., Liu, S., Johnson, A. C., Sweetman, A. J., and Baninla, Y.: Pollution pathways and

409   release estimation of perfluorooctane sulfonate (PFOS) and perfluorooctanoic acid (PFOA) in central and eastern China,

410   Sci. Total Environ., 580, 1247-1256, https://doi.org/10.1016/j.scitotenv.2016.12.085, 2017.

411   Martin, J. W., Ellis, D. A., Mabury, S. A., Hurley, M. D., and Wallington, T. J.: Atmospheric chemistry of

412   perfluoroalkanesulfonamides: kinetic and product studies of the OH radical and Cl atom initiated oxidation of N-ethyl

413   perfluorobutanesulfonamide, Environ. Sci. Technol., 40, 864-872, https://doi.org/10.1021/es051362f, 2006.

414   Pavlína, K., Garry, C., Lisa, M., and Jana, K.: A critical assessment of passive air samplers for per- and polyfluoroalkyl

415   substances, Atmos. Environ., 185, 186-195, https://doi.org/10.1016/j.atmosenv.2018.05.030, 2018.

416   Pickard H. M., Criscitiello A. S., Spencer C., Sharp M. J., Muir D.C. G., De Silva A. O., Young C. J.: Continuous

417   non-marine inputs of per- and polyfluoroalkyl substances to the High Arctic: a multi-decadal temporal record, Atmos.

418   Chem. Phys., 18, 5045–5058, https://doi.org/10.5194/acp-18-5045-2018, 2018.

419   Rauert, C., Harner, T., Schuster, J. K., Eng, A., Fillmann, G., Castillo, L. E., Fentanes, O., Villa, M. I., Miglioranza, K.,

420   and Moreno, I. R.: Atmospheric Concentrations of New Persistent Organic Pollutants and Emerging Chemicals of

421   Concern in the Group of Latin America and Caribbean (GRULAC) Region, Environ. Sci. Technol., 52(13), 7240-7249,

422   https://doi.org/ 10.1021/acs.est.8b00995, 2018.

423   Thackray, C. P., Selin N. E.: Uncertainty and variability in atmospheric formation of PFCAs from fluorotelomer

424   precursors, Atmos. Chem. Phys., 17, 4585–4597, https://doi:10.5194/acp-17-4585-2017, 2017.

425   Tian, Y., Yao, Y., Chang, S., Zhao, Z., Zhao, Y., Yuan, X., Wu, F., and Sun, H.: Occurrence and Phase Distribution of

426   Neutral and Ionizable Per- and Polyfluoroalkyl Substances (PFASs) in the Atmosphere and Plant Leaves around Landfills:

427   A Case Study in Tianjin,China, Environ. Sci. Technol., 52, 1301-1310, https://doi.org/10.1021/acs.est.7b05385, 2018.

428   Wang, Q. W., Yang, G. P., Zhang, Z. M., and Jian, S.: Perfluoroalkyl acids in surface sediments of the East China Sea,

429   Environ. Pollut., 231, 59-67, https://doi.org/10.1016/j.envpol.2017.07.078, 2017.

430   Wang, Z., Cousins, I. T., Scheringer, M., Buck, R. C., and Hungerbühler, K.: Global emission inventories for C4-C14

431   perfluoroalkyl carboxylic acid (PFCA) homologues from 1951 to 2030, Part I: production and emissions from

432   quantifiable sources, Environ. Int., 70, 62–75, https://doi.org/10.1016/j.envint.2014.04.013, 2014.

433   Wang X., Schuster J., Jones K. C., Gong P.:Occurrence and spatial distribution of neutral perfluoroalkyl substances and

434   cyclic volatile methylsiloxanes in the atmosphere of the Tibetan Plateau, Atmos. Chem. Phys., 18, 8745–8755,

435   https://doi.org/10.5194/acp-18-8745-2018, 2018.

436   Wong, F., Shoeib, M., Katsoyiannis, A., Eckhardt, S., Stohl, A., Bohlinnizzetto, P., Li, H., Fellin, P., Su, Y., and Hung, H.:

437   Assessing temporal trends and source regions of per- and polyfluoroalkyl substances (PFASs) in air under the Arctic

438   Monitoring   and   Assessment   Programme   (AMAP),   Atmos.   Environ.,   172,   65-73,   https://doi.org/

439   10.1016/j.atmosenv.2017.10.028, 2018.

440   Xie, S., Wang, T., Liu, S., Jones, K. C., Sweetman, A. J., and Lu, Y.: Industrial source identification and emission

441   estimation of perfluorooctane sulfonate in China, Environ. Int., 52, 1-8, https://doi.org/10.1016/j.envint.2012.11.004,

442   2013.

443   Yao, Y., Chang, S., Sun, H., Gan, Z., Hu, H., Zhao, Y., and Zhang, Y.: Neutral and ionic per- and polyfluoroalkyl

444   substances (PFASs) in atmospheric and dry deposition samples over a source region (Tianjin, China), Environ Pollut, 212,

445   449-456, https://doi.org/10.1016/j.envpol.2016.02.023, 2016a.

446   Yao, Y., Sun, H., Gan, Z., Hu, H., Zhao, Y., Chang, S., and Zhou, Q. X.: A Nationwide Distribution of Per- and

447   Polyfluoroalkyl Substances (PFASs) in Outdoor Dust in Mainland China From Eastern to Western Areas, Environ. Sci.

448   Technol., 50(7), 3676-3685, https://doi.org/10.1021/acs.est.6b00649, 2016b.